Modeling Viscoelasticity and Dynamic Nematic Order of Exchangeable Liquid Crystal Elastomers

Jiameng Zhao[1,2] and Fanlong Meng[1,2,3,*]

[1]CAS Key Laboratory of Theoretical Physics, Institute of Theoretical Physics, Chinese Academy of Sciences, Beijing 100190, China
[2]School of Physical Sciences, University of Chinese Academy of Sciences, Beijing 100049, China
[3]Wenzhou Institute, University of Chinese Academy of Sciences, Wenzhou, Zhejiang 325000, China

(Received 1 January 2023; accepted 26 April 2023; published 11 August 2023)

Exchangeable liquid crystal elastomers (XLCEs), an emerging class of recyclable polymer materials, consist of liquid crystalline polymers which are dynamically crosslinked. We develop a macroscopic continuum model by incorporating the microscopic dynamic features of the cross-links, which can be utilized to understand the viscoelasticity of the materials together with the dynamic nematic order. As applications of the model, we study the rheological responses of XLCEs in three cases: stress relaxation, strain ramp, and creep compliance, where the materials show interesting rheology as an interplay between the dynamic nematic order of the mesogenic units, the elasticity from the network structure, and the dissipation due to chain exchange reactions. Not only being useful in understanding the physical mechanism underlying the fascinating characteristics of XLCEs, this work can also guide their future fabrications with desired rheological properties.

DOI: 10.1103/PhysRevLett.131.068101

In liquid crystal elastomers (LCEs), the coupling between the macroscopic shape change and the alignment of the microscopic mesogenic units offers the possibility of performing mechanical works by tuning the orientational order of the mesogenic units, which was first proposed by de Gennes in 1975 as a competitive candidate of thermotropic mechanical actuators [1]. A well-aligned monodomain LCE possesses very attractive mechanical properties [2–5], e.g., reversible large strain deformations, high strength, and excellent toughness, and LCEs can exhibit interesting "soft elasticity" (zero stress for material deformation) due to the coupling between the polymer elasticity and the nematic order [6,7]. Because of such physical properties, LCEs can serve as actuators [8–10], dampers [6,11], adhesives [12,13], etc. Nevertheless, the difficulties in achieving a uniform alignment of the mesogenic units due to the random quenched disorder [14,15] and the nonrecyclability of the material as other common thermosets [16,17] hinder wide applications of LCEs in industry.

In order to overcome such shortcomings of LCEs, the first exchangeable liquid crystal elastomer (XLCE) was synthesized in 2014, where the permanent cross-links in LCEs are replaced by dynamic ones based on the transesterification reaction allowing the network to rearrange its topology (illustrated in Fig. 1) [18]. After this, various XLCEs are fabricated in laboratories by utilizing different dynamic covalent chemistry techniques (transesterification [19–21], Diels-Alder reaction [22], disulfide exchange [23], etc.) to implement the bond exchange reaction in XLCEs, which have been recently reviewed in Ref. [24]. Depending on the dynamics of the bond exchange reaction, XLCEs can be categorized into associative (new bonds form first and then old bonds break) and dissociative (old bonds break first and then new bonds form) ones as for other covalently adaptive networks; the associative XLCEs can easily maintain the integrity compared with the dissociative ones because the crosslink number in associative XLCEs is conserved while that in dissociative ones can decrease with time. The introduction of the chain exchange reactions in XLCEs makes it possible to fabricate macroscopic LCEs with perfect nematic alignment (first achieving perfect alignment in XLCEs by mechanical loading or applying external fields at high temperatures at which chain exchange reactions can easily happen, and then quenching the material to the room temperature or other temperatures

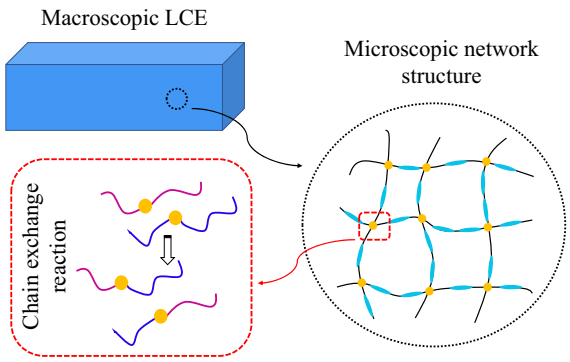

FIG. 1. A main-chain XLCE consists of liquid crystalline polymers [the mesogenic units (cyan) are embedded into the flexible polymer backbone], where the polymers are dynamically crosslinked by covalent bonds (yellow dots).

in applications), and now XLCEs are treated with significant potentials for industrial applications. However, despite the remarkable experimental advances in fabricating different XLCEs and the promising potentials of their future applications, a theoretical framework for understanding the rheology of XLCEs is still absent, mainly due to the complexity in the coupling between the dynamically evolving nematic order, the entropic elasticity of the polymeric material, and the dissipation due to chain exchange reactions.

In this Letter, we construct a macroscopic continuum model of XLCEs, in which the microscopic dynamics of the cross-links are incorporated. Based on this model, the viscoelasticity and the dynamic nematic order of XLCEs can be analyzed, for which three common rheology tests are shown: stress relaxation, strain ramp, and creep compliance.

Theoretical framework.—We shall consider associative XLCEs in the following, which possess a constant number of cross-links maintaining the integrity of the materials. In such XLCEs, the bond exchange reaction resembles that in vitrimers (a class of associative covalent adaptive networks without mesogenic units [25,26]), which happens with the rate $\beta = \omega_0 \exp[-W_e/k_B T]$ [27–29], where ω_0 denotes the thermal fluctuating frequency and W_e denotes the energy barrier of the bond exchange reaction. In certain cases, forces acting on the crosslinked polymers can also influence the bond exchange rate [30–32], and here we ignore such mechanochemical effect for seeking the transparency of the theory. Note that we would not consider other relaxation modes, e.g., Rouse relaxation, in this work for simplicity, whose timescale is usually well separated from that of the chain exchange reactions for most of the XLCEs fabricated in laboratories currently but can be comparable in certain cases. The newly crosslinked polymers at the moment of the bond exchange reaction are assumed to be in their relaxed state, i.e., the reference states of both the polymers and the associated mesogenic units depend on the time when bond exchange reactions happen.

Similarly with ordinary vitrimers of which the polymers can also dynamically break from and re-cross-link to the cross-links, the total number of the crosslinked chains in XLCEs can be expressed as [27]

$$N(t) = N_0 e^{-\beta t} + N_0 \int_0^t dt' \beta e^{-\beta(t-t')}, \tag{1}$$

where N_0 denotes the number of the crosslinked chains at time $t = 0$, the first term on the right-hand side denotes the number of the crosslinked chains which are crosslinked at time $t = 0$ and remain crosslinked until time t, and the second term denotes the chains which are crosslinked at different time $t' > 0$ and remain crosslinked until time t. Obviously, the total number of crosslinked chains is a constant $N(t) \equiv N_0$, one of the key features of associative XLCEs.

Since the reference states of the polymers and the mesogenic units are defined when they are crosslinked, the free energy density of an XLCE can be expressed as

$$\mathcal{F}_{\mathrm{XLCE}}(t) = e^{-\beta t} F_{\mathrm{LCE}}(t;0) + \int_0^t dt' \beta e^{-\beta(t-t')} F_{\mathrm{LCE}}(t;t'), \tag{2}$$

where $F_{\mathrm{LCE}}(t;t')$ denotes the free energy density of the permanently crosslinked XLCE at time t (i.e., LCE), referenced at its crosslinking time t'. In other words, an XLCE can be treated as a set of LCEs prepared with different reference states. In the following, we shall take nematic XLCEs which are the most common class fabricated in laboratories for illustrating the dynamic features of XLCEs. The free energy density of a permanently crosslinked LCE, $F_{\mathrm{LCE}} = F_{\mathrm{pol}} + F_{\mathrm{nem}}$, consists of the contributions from both the polymer elasticity and the nematic elasticity [4]. Suppose the deformation gradient tensor is $\boldsymbol{E}$, and the mesogenic units form nematics where the nematic tensor is $\boldsymbol{Q} = Q(3\hat{\boldsymbol{n}}\hat{\boldsymbol{n}} - \boldsymbol{\delta})/2$ with Q as the nematic order parameter and $\hat{\boldsymbol{n}}$ as the nematic director. Then the polymer elasticity of incompressible XLCEs can be described by the neoclassical theory [4,33], $F_{\mathrm{pol}} = (G/2)\{\mathrm{Tr}(\boldsymbol{\ell}_0 \cdot \boldsymbol{E}^T \cdot \boldsymbol{\ell}^{-1} \cdot \boldsymbol{E}) + \ln[\mathrm{Det}(\boldsymbol{\ell})/\mathrm{Det}(\boldsymbol{\ell}_0)]\}$ with G as the shear modulus, and $\boldsymbol{\ell}_0$ and $\boldsymbol{\ell}$ as the step length tensor before and after the deformation, respectively. $\boldsymbol{\ell}_0$ and $\boldsymbol{\ell}$ are not unit tensors due to the presence of the mesogenic units, and the values depend on the nematic order parameter Q; for LCE of freely joint main chain polymers, there is a simple relation: $\boldsymbol{\ell} = a(\boldsymbol{\delta} + 2\boldsymbol{Q})$ with a as the length of one mesogenic unit [4], and this will be taken in the following discussions. For nematic elasticity, we simply take the Landau-de Gennes model, $F_{\mathrm{nem}} = A\,Q^2/2 - B\,Q^3/3 + C\,Q^4/4$ with the coefficients A, B, and C with the same dimension of the elastic modulus [34]; in this Letter, we take a fixed and reasonable parameter set for describing the nematic elasticity: $A = 20G$, $B = 4G$, and $C = 30G$, without losing generality of the discussions. The effect of the spatial gradient of the nematic order as described by Frank energy [35] is neglected in this continuum model, and such approximation is fine when the characteristic length of the material exceeds the nematic penetration length of XLCEs/LCEs [4], $\xi = \sqrt{K/G} \sim$ 10 nm, where K and G are the Frank constant and the shear modulus of the material, respectively; the spatial gradient of the nematic order can be important when there are nanoscaled orientational patterns formed in the materials, which will not be discussed in this Letter.

We shall discuss the responses of XLCEs subjected to a uniaxial stretch in the following, in order to demonstrate the rheological properties of XLCEs quantitatively. The deformation gradient tensor of the uniaxial stretch along the x axis which is referenced at time $t = 0$ is $\boldsymbol{E}(t;0) = \mathrm{Diag}[\lambda(t), 1/\sqrt{\lambda(t)}, 1/\sqrt{\lambda(t)}]$, where $\lambda(t)$ denotes the elongation ratio of the sample along the x axis. For the chains

crosslinked at time t', the deformation gradient tensor in the neoclassical theory is $\boldsymbol{E}(t;t') = \boldsymbol{E}(t;0)\cdot\boldsymbol{E}^{-1}(t';0)$, correspondingly. Meanwhile, for the chains crosslinked at time t', they can have their initial nematic order defined as $Q(t') = Q_0$ satisfying $\partial F_{\rm nem}/\partial Q|_{Q_0} = 0$; note that Q_0 does not depend on the deformation history of the materials, which is different from the reference state of the mechanical part defined based on the deformation history. We shall focus on the case of $Q_0 = 0$ in this Letter which stands for XLCEs whose vitrification temperature is higher than the nematic-isotropic transition temperature, i.e., $T_{\rm v} > T_{\rm ni}$, mainly in order to avoid the possible complexity of the polydomains in LCEs. The adiabatic approximation for the chains crosslinked at different time is taken, i.e., the nematic order of the chains only evolves with their own experienced deformations rather than being influenced by others, which works well when polymers in the network are not dense. Then at time t, the nematic order of the chains crosslinked at time t' can be expressed as $Q(t;t')$. Without any direct manipulations on the nematics, e.g., by applying an electric field, the nematic order of the sample can be determined at given deformations, by $\delta\mathcal{F}_{\rm XLCE}(t)/\delta Q(t;t') = 0$, which defines the coupling between the nematic order $Q(t;t')$ and the mechanical loading $\boldsymbol{E}(t;t')$ (see Supplemental Material [36]). Then we can obtain the constitutive relation by $\sigma(t) = \partial\mathcal{F}_{\rm XLCE}(t)/\partial\lambda(t)$, as

$$\frac{\sigma(t)}{G} = e^{-\beta t}\left[\lambda(t)\frac{\ell^0_\parallel}{\ell_\parallel(t;0)} - \frac{1}{\lambda^2(t)}\frac{\ell^0_\perp}{\ell_\perp(t;0)}\right] + \int_0^t dt'\beta e^{-\beta(t-t')}\left[\frac{\lambda(t)}{\lambda^2(t')}\frac{\ell^0_\parallel}{\ell_\parallel(t;t')} - \frac{\lambda(t')}{\lambda^2(t)}\frac{\ell^0_\perp}{\ell_\perp(t;t')}\right], \tag{3}$$

where $\ell_\perp(t;t) = a[1-Q(t;t)]$ and $\ell_\parallel(t;t) = a[1+2Q(t;t)]$ denote the component of the step length tensor (diagonal) in the parallel and perpendicular direction regarding the stretch, respectively. For ordinary vitrimers, i.e., without the nematic order, one can simply take $\ell_\perp = \ell_\parallel = a$ in Eq. (3) to calculate the responses of vitrimers [28], which will be used for comparisons between XLCEs and vitrimers in the following discussions. Meanwhile, the total nematic order of the XLCEs, one of the most characteristic features, can be obtained by

$$Q_{\rm tot}(t) = e^{-\beta t}Q(t;0) + \int_0^t dt'\beta e^{-\beta(t-t')}Q(t;t') \tag{4}$$

by summing up the contributions from all crosslinked polymers. Obviously, the constitutive relation [Eq. (3)] denoting the viscoelastic properties of the XLCEs is coupled with the dynamic evolution of the nematic order [Eq. (4)], which is the key for understanding the differences in the viscoelastic responses between XLCEs and vitrimers. Based on the above theoretical framework, we shall discuss the responses of XLCEs in three common rheology tests: stress relaxation, strain ramp, and creep compliance.

Stress relaxation.—In a stress relaxation measurement, the sample of the reference state ($\lambda_0 = 1$, $Q_0 = 0$) is stretched instantaneously at time $t = 0$ with the stretch ratio $\lambda_{\rm I}$ (strain as $\varepsilon_{\rm I} = \lambda_{\rm I} - 1$) along the $\boldsymbol{e}_x$ direction, and then the mesogenic units, randomly oriented at the beginning, are also along the same direction now due to the stretch. Simultaneously, the nematic order of the XLCE will increase to $Q_{\rm I}$ by optimizing the free energy of liquid crystal elastomers, which is $Q_{\rm I} = \kappa(\lambda_{\rm I} - 1)$ for $\lambda_{\rm I} \to 1$ with $\kappa = 3/[A(T)+3]$ (see the Supplemental Material [36]). By keeping the stretch ratio as $\lambda_{\rm I}$, it is obvious from Eq. (3) that the tensile stress relaxes exponentially with time (see the comparison with experiments in Fig. 2), $\sigma(t)/G = e^{-\beta t}[\lambda_{\rm I}\ell^0_\parallel/\ell^{\rm I}_\parallel - \ell^0_\perp/(\lambda^2_{\rm I}\ell^{\rm I}_\perp)]$ with $\ell^{0,{\rm I}}_\parallel = a[1+2Q_{0,{\rm I}}]$ and $\ell^{0,{\rm I}}_\perp = a[1-Q_{0,{\rm I}}]$, since the second term on the right-hand side of Eq. (3) does not contribute due to the fact that the current deformation state (with stretch ratio $\lambda_{\rm I}$) is identical to the reference state (being crosslinked with stretch ratio $\lambda_{\rm I}$). Meanwhile, the nematic order of the XLCE also decays exponentially due to the chain exchange reaction, $Q(t) = Q_{\rm I}e^{-\beta t}$, which is illustrated in Fig. 2. In experiments, the stress can relax in the form of the stretched exponential function, i.e., $e^{-(\beta t)^\alpha}$ with $0 < \alpha < 1$ as the stretch factor whose value can depend on the polydispersity of the energy barriers for the chain exchange reaction [31], mesh sizes [43], etc. In this case, one needs to change the single exponential-decaying prefactor $e^{-\beta t}$ and the memory kernel $e^{-\beta(t-t')}$ in Eqs. (1) and (2) to the ones incorporating the distribution of all relaxation modes, and interested readers can refer to the Supplemental Material [36].

Strain ramp.—Consider an XLCE subjected to a ramp deformation, i.e., the elongation ratio (thus the applied strain) increases linearly with time, $\lambda(t) = 1 + \dot\gamma t$ with $\dot\gamma$ as

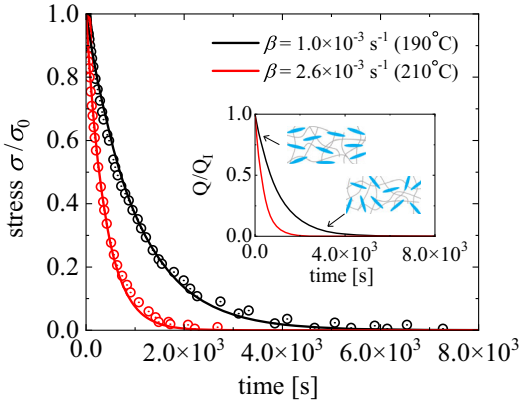

FIG. 2. Stress relaxation of XLCEs, with the dots extracted from the experiments [18] and the solid lines fitted by the equation $\sigma(t)/\sigma_0 = e^{-\beta t}$ (the inset denotes the accompanying relaxation of the nematic order).

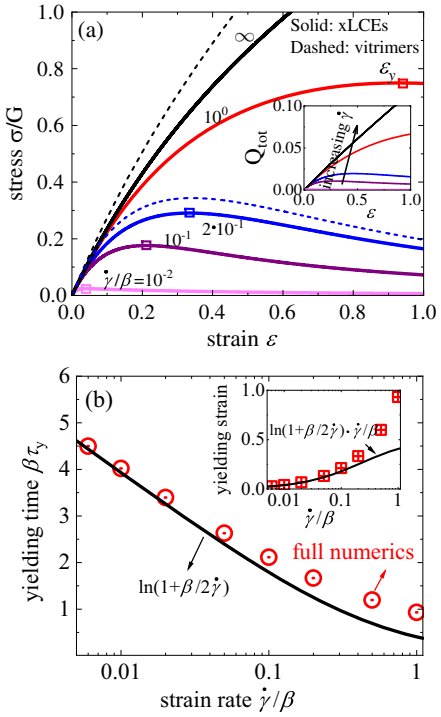

FIG. 3. (a) Stress-strain relations of XLCEs (solid lines with the strain rate $\dot\gamma/\beta = 0.01$, 0.1, 0.2, 1, and ∞) and vitrimers (dashed lines with $\dot\gamma/\beta = 0.2$ and ∞ as two examples for comparison). Square dots on the curves denote the yielding points where the stress starts decreasing with the strain. Inset shows how the total nematic order of XLCEs changes with the strain. (b) Dependence of the yielding time $\beta\tau_y$ on the applied strain rate $\dot\gamma/\beta$ (both with the time unit defined by $1/\beta$) of XLCEs, and the inset shows the relations between the yielding strain $\dot\gamma\tau_y$ and the strain rate $\dot\gamma/\beta$. The dots denote the numerical results, and the lines denote the analytic relation shown in Eq. (5).

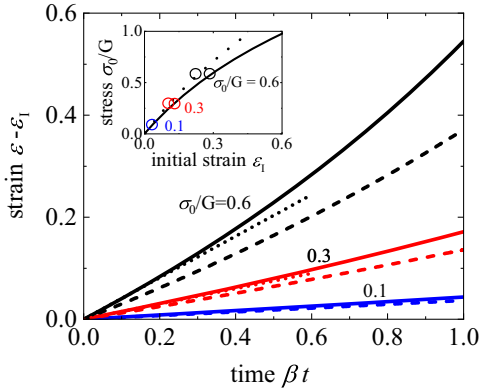

FIG. 4. Strain evolution of XLCEs in tests of creep compliance. Solid lines denote the numerical results by solving Eq. (3) for XLCEs with applied stress of $\sigma_0/G = 0.6$, 0.3, and 0.1; dashed lines denote the numerical results of ordinary vitrimers for comparisons; and dotted lines denote the results of linear viscoelasticity given by Eq. (6). The inset shows the relationship between the initial strain and the applied stress (solid line for XLCEs and dotted line for vitrimers).

the constant strain rate. During such a stretch process, the stress develops with the strain following the constitutive relation [Eq. (3)], and the information of the total nematic order can be obtained by Eq. (4). As illustrated in Fig. 3(a), the stress-strain curves of XLCEs obviously lie below those of vitrimers which are stretched with the same strain rate, due to the feedback of the increased nematic order (induced by the stretch) in the stress-strain relation. In Fig. 3(a), the stress of XLCEs first increases and then decreases with the stress, where the increase is due to the natural elasticity of the networked material before the occurrence of a significant amount of chain exchange reactions, and the decrease is due to the memory loss by the chain exchange reactions.

We introduce yielding time τ_y defined by $d\sigma/dt|_{\tau_y} = 0$ and the yielding strain as $\varepsilon_y = \dot\gamma\tau_y$ to characterize when such elasticity-plasticity transitions happen. Note that the total nematic order exhibits a similar response with the stress, but the yielding strain for the nematic order ε_y^Q is larger than that defined in the stress-strain curves, ε_y [shown in the inset of Fig. 3(a)]. With the increase of the strain rate, yielding time τ_y decreases while the yielding strain ε_y increases, which can be obtained by numerically solving Eq. (3) and is shown in Fig. 3(b). Alternatively, one can simply take an approximate relation between the nematic order with the applied strain: $Q(t;t') = \kappa\,\varepsilon(t;t')$ (see the Supplemental Material [36]) and expand the stress-strain relationship in terms of ε and ε^2 before taking the time integral, and then the relationship between the yielding time and the strain rate can be obtained as

$$\tau_y \simeq \frac{1}{\beta}\ln(1+\beta/2\dot\gamma). \tag{5}$$

For $\dot\gamma/\beta \ll 1$, this simple relation matches very well with the full numerical calculations [shown in Fig. 3(b)] and Eq. (5) can be expressed as $\tau_y \simeq \frac{1}{\beta}\ln(1+\beta/2\dot\gamma - \kappa\ln\kappa)$ for large κ].

Creep compliance.—By exerting a constant tensile stress σ_0 on an XLCE, the material will instantaneously elongate with an initial strain ε_I as in the stress relaxation measurements; such a stress-strain relation is shown in the inset of Fig. 4. Three stress values are taken to show the creep compliance of XLCEs, $\sigma_0/G = 0.1$, 0.3, and 0.6. Obviously from Fig. 4, the strain first increases with time in the linear manner after the instantaneous strain ε_I and then accelerates in long time response, which is named as strain thinning in rheology. Also, the nematic order responds similarly to the strain (not shown here), i.e., Q first increases linearly and then accelerates.

In order to quantitatively measure the strain evolution of XLCEs in the short time limit, we can define an effective viscosity: $\eta_0 = \sigma_0 \cdot (\frac{d\varepsilon}{dt}|_{t=0})^{-1}$. By expanding the strain in the short time limit $\varepsilon(t) = \varepsilon_I + \mathcal{A}t + \mathcal{O}[(\beta t)^2]$ and

imposing the stress in Eq. (3) as the constant σ_0, then we can obtain

$$\eta_0 = \sigma_0 \cdot \mathcal{A}^{-1} \simeq [\beta\varepsilon_{\mathrm{I}} + \beta(1+\kappa)\varepsilon_{\mathrm{I}}^2]^{-1}, \tag{6}$$

which shows that the effective viscosity decreases with the applied strain or the stress. Such a simple linear relation $\varepsilon(t \to 0) - \varepsilon_0 = \mathcal{A}t$ nicely captures the initial stage of the creep compliance of XLCEs (dotted curves in Fig. 4). Note that the strain of XLCEs is larger than that of ordinary vitrimers under the same condition (time and stress), which results again from the coupling between the nematic order and the mechanical properties in XLCEs. Resembling the response of ordinary vitrimers [28], the effective viscosity of XLCEs decreases with time (or strain), exhibiting strain thinning behaviors due to the mechanical memory loss arising from chain exchange reactions. Note that it is also possible for XLCEs to exhibit strain thickening responses for large deformations due to finite stretchability of the materials [44], for which one needs to replace the neo-classical model of F_{pol} with the one incorporating finite stretchability of the materials.

In conclusion, we construct a macroscopic continuum model for describing the viscoelastic properties of XLCEs, by incorporating the microscopic dynamics of the chain exchange reactions and the dynamic evolution of the nematic order. By applying the model, we show how XLCEs respond in typical rheology tests, including stress relaxation, ramp deformation, and creep compliance, where the coupling between the mechanic properties of the crosslinked network and the nematic order endows XLCEs with very fascinating rheological responses. This portable model can be easily generalized to analyze the rheology of XLCEs in other deformation circumstances, e.g., oscillatory shear and biaxial stretch-compression, XLCEs with nonzero initial nematic orders, or even for XLCEs with more complex network structures such as double-networked ones. We also hope that this theoretical work can guide future industrial fabrications of XLCEs with designed viscoelastic properties.

This work is supported by National Natural Science Foundation of China (Grant No. 12275332 and 12047503), Chinese Academy of Sciences, and Wenzhou Institute (Grant No. WIUCASICTP2022). The computations of this work were conducted on the HPC cluster of ITP-CAS.

*fanlong.meng@itp.ac.cn

[1] P. De Gennes, Réflexions sur un type de polymères nématiques, CR Acad. Sci. Ser. B **281**, 101 (1975).
[2] J. V. Selinger, H. G. Jeon, and B. R. Ratna, Isotropic-Nematic Transition in Liquid-Crystalline Elastomers, Phys. Rev. Lett. **89**, 225701 (2002).
[3] A. Lebar, Z. Kutnjak, S. Žumer, H. Finkelmann, A. Sánchez-Ferrer, and B. Zalar, Evidence of Supercritical Behavior in Liquid Single Crystal Elastomers, Phys. Rev. Lett. **94**, 197801 (2005).
[4] M. Warner and E. M. Terentjev, *Liquid Crystal Elastomers* (Oxford University Press, New York, 2007), Vol. 120.
[5] T. J. White and D. J. Broer, Programmable and adaptive mechanics with liquid crystal polymer networks and elastomers, Nat. Mater. **14**, 1087 (2015).
[6] S. Clarke, A. Tajbakhsh, E. Terentjev, C. Remillat, G. Tomlinson, and J. House, Soft elasticity and mechanical damping in liquid crystalline elastomers, J. Appl. Phys. **89**, 6530 (2001).
[7] O. Stenull and T. C. Lubensky, Phase Transitions and Soft Elasticity of Smectic Elastomers, Phys. Rev. Lett. **94**, 018304 (2005).
[8] O. M. Wani, H. Zeng, and A. Priimagi, A light-driven artificial flytrap, Nat. Commun. **8**, 15546 (2017).
[9] A. Kotikian, C. McMahan, E. C. Davidson, J. M. Muhammad, R. D. Weeks, C. Daraio, and J. A. Lewis, Untethered soft robotic matter with passive control of shape morphing and propulsion, Sci. Rob. **4**, eaax7044 (2019).
[10] Y. Zhang, Z. Wang, Y. Yang, Q. Chen, X. Qian, Y. Wu, H. Liang, Y. Xu, Y. Wei, and Y. Ji, Seamless multimaterial 3d liquid-crystalline elastomer actuators for next-generation entirely soft robots, Sci. Adv. **6**, eaay8606 (2020).
[11] M. O. Saed, W. Elmadih, A. Terentjev, D. Chronopoulos, D. Williamson, and E. M. Terentjev, Impact damping and vibration attenuation in nematic liquid crystal elastomers, Nat. Commun. **12**, 6676 (2021).
[12] J. Cui, D.-M. Drotlef, I. Larraza, J. P. Fernández-Blázquez, L. F. Boesel, C. Ohm, M. Mezger, R. Zentel, and A. del Campo, Bioinspired actuated adhesive patterns of liquid crystalline elastomers, Adv. Mater. **24**, 4601 (2012).
[13] T. Ohzono, M. O. Saed, and E. M. Terentjev, Enhanced dynamic adhesion in nematic liquid crystal elastomers, Adv. Mater. **31**, 1902642 (2019).
[14] S. Clarke, E. Nishikawa, H. Finkelmann, and E. Terentjev, Light-scattering study of random disorder in liquid crystalline elastomers, Macromol. Chem. Phys. **198**, 3485 (1997).
[15] L. Petridis and E. M. Terentjev, Nematic-isotropic transition with quenched disorder, Phys. Rev. E **74**, 051707 (2006).
[16] S. Thomas and R. Stephen, *Rubber Nanocomposites: Preparation, Properties, and Applications* (John Wiley & Sons, New York, 2010).
[17] M. Morton, *Rubber Technology* (Springer Science & Business Media, New York, 2013).
[18] Z. Pei, Y. Yang, Q. Chen, E. M. Terentjev, Y. Wei, and Y. Ji, Mouldable liquid-crystalline elastomer actuators with exchangeable covalent bonds, Nat. Mater. **13**, 36 (2014).
[19] X. Lu, S. Guo, X. Tong, H. Xia, and Y. Zhao, Tunable photocontrolled motions using stored strain energy in malleable azobenzene liquid crystalline polymer actuators, Adv. Mater. **29**, 1606467 (2017).
[20] D. W. Hanzon, N. A. Traugutt, M. K. McBride, C. N. Bowman, C. M. Yakacki, and K. Yu, Adaptable liquid crystal elastomers with transesterification-based bond exchange reactions, Soft Matter **14**, 951 (2018).
[21] A. Gablier, M. O. Saed, and E. M. Terentjev, Transesterification in epoxy–thiol exchangeable liquid crystalline elastomers, Macromolecules **53**, 8642 (2020).

[22] Z.-C. Jiang, Y.-Y. Xiao, L. Yin, L. Han, and Y. Zhao, Self-lockable liquid crystalline Diels–Alder dynamic network actuators with room temperature programmability and solution reprocessability, Angew. Chem. **132**, 4955 (2020).
[23] Z. Wang, H. Tian, Q. He, and S. Cai, Reprogrammable, reprocessible, and self-healable liquid crystal elastomer with exchangeable disulfide bonds, ACS Appl. Mater. Interfaces **9**, 33119 (2017).
[24] M. O. Saed, A. Gablier, and E. M. Terentjev, Exchangeable liquid crystalline elastomers and their applications, Chem. Rev. **122**, 4927 (2022).
[25] D. Montarnal, M. Capelot, F. Tournilhac, and L. Leibler, Silica-like malleable materials from permanent organic networks, Science **334**, 965 (2011).
[26] W. Denissen, J. M. Winne, and F. E. D. Prez, Vitrimers: Permanent organic networks with glass-like fluidity, Chem. Sci. **7**, 30 (2016).
[27] F. Meng, M. O. Saed, and E. M. Terentjev, Elasticity and relaxation in full and partial vitrimer networks, Macromolecules **52**, 7423 (2019).
[28] F. Meng, M. O. Saed, and E. M. Terentjev, Rheology of vitrimers, Nat. Commun. **13**, 5753 (2022).
[29] F. Tanaka and S. F. Edwards, Viscoelastic properties of physically crosslinked networks. 1. Transient network theory, Macromolecules **25**, 1516 (1992).
[30] F. Tanaka and S. Edwards, Viscoelastic properties of physically crosslinked networks, J. Non-Newtonian Fluid Mech. **43**, 247 (1992).
[31] F. Meng, R. H. Pritchard, and E. M. Terentjev, Stress relaxation, dynamics, and plasticity of transient polymer networks, Macromolecules **49**, 2843 (2016).
[32] Y. Yang, E. M. Terentjev, Y. Wei, and Y. Ji, Solvent-assisted programming of flat polymer sheets into reconfigurable and self-healing 3d structures, Nat. Commun. **9**, 1906 (2018).
[33] P. Bladon, E. M. Terentjev, and M. Warner, Transitions and instabilities in liquid crystal elastomers, Phys. Rev. E **47**, R3838 (1993).
[34] P.-G. De Gennes and J. Prost, *The Physics of Liquid Crystals* (Oxford University Press, New York, 1993), p. 83.
[35] J. V. Selinger, Interpretation of saddle-splay and the Oseen-Frank free energy in liquid crystals, Liq. Cryst. Rev. **6**, 129 (2018).
[36] See Supplemental Material at http://link.aps.org/supplemental/10.1103/PhysRevLett.131.068101 for more details of free energy minimization, nematic order, stetched-exponential type stress relaxation and creep compliance, which includes Refs. [37–42].
[37] J. Phillips, Stretched exponential relaxation in molecular and electronic glasses, Rep. Prog. Phys. **59**, 1133 (1996).
[38] D. C. Johnston, Stretched exponential relaxation arising from a continuous sum of exponential decays, Phys. Rev. B **74**, 184430 (2006).
[39] P. Humbert, Nouvelles correspondances symboliques, Bull. Sci. Math. **69**, 121 (1945).
[40] H. S. Pollard, The representation of e^{-x^λ} as a Laplace integral, Bull. Am. Math. Soc. **52**, 908 (1946).
[41] Y. Serero, V. Jacobsen, J.-F. Berret, and R. May, Evidence of nonlinear chain stretching in the rheology of transient networks, Macromolecules **33**, 1841 (2000).
[42] A. Hotta, S. Clarke, and E. Terentjev, Stress relaxation in transient networks of symmetric triblock styrene-isoprene- styrene copolymer, Macromolecules **35**, 271 (2002).
[43] F. Meng and E. M. Terentjev, Fluidization of transient filament networks, Macromolecules **51**, 4660 (2018).
[44] F. Meng and E. M. Terentjev, Transient network at large deformations: Elastic–plastic transition and necking instability, Polymers **8**, 108 (2016).